Differential Effects of Mg^{2+} Ions on the Individual Kinetic Steps of Human Cytosolic and Mitochondrial Aldehyde Dehydrogenases†

Kwok Ki Ho,‡,§ Abdellah Allali-Hassani,‡,§ Thomas D. Hurley,|| and Henry Weiner*,‡

Department of Biochemistry, Purdue University, West Lafayette, Indiana 47907-1153, and Department of Biochemistry and Molecular Biology, Indiana University School of Medicine, Indianapolis, Indiana 46202-5122

Received January 7, 2005; Revised Manuscript Received March 22, 2005

ABSTRACT: Although the structures of mammalian cytosolic and mitochondrial ALDH have been determined, several differences, mainly functional, between these two 70% identical isozymes remain unexplained. A major difference is the differential effect of Mg^{2+} ions that inhibits the cytosolic and activates the mitochondrial isozyme. Here, we have investigated the effect of Mg^{2+} ions on each individual kinetic step of ALDH1 and ALDH2. The metal ions were found not to affect either acylation or hydride transfer for either isozyme. The lack of a Mg^{2+} ion effect on hydride transfer was further demonstrated with an E399Q mutant of ALDH1 whose rate-limiting step had been changed from NADH dissociation to hydride transfer. The other steps, however, were affected by Mg^{2+} ions for both isozymes. The metal ions inhibited NADH dissociation, the rate-limiting step for ALDH1, and enhanced deacylation, the rate-limiting step for ALDH2. Our results indicated that, with both isozymes, Mg^{2+} ions tightened the binding of NADH, and by binding to the coenzyme, they increased the nucleophilicity of the nucleophile Cys302. The inhibition of ALDH1 and activation of ALDH2 at pH 7.4 are due to their different rate-limiting steps. Mg^{2+} ions affected similarly the NADH activation of the esterase reaction for both isozymes. In contrast, the metal ions affected only the NAD^+ activation of ALDH1. This latter finding and other features described here can be rationalized on the basis of the known three-dimensional structures of the isozymes.

It has been known for some time that divalent cations such as Mg^{2+}, Mn^{2+}, and Ca^{2+} affect differently the three major isozymes of mammalian ALDH.[1] These ions appear to increase the specific activity of the tetrameric mitochondrial (class 2) isozyme (*1*−*3*), inhibit the tetrameric cytosolic (class 1) isozyme (*4*−*6*), and have no effect on the dimeric cytosolic (class 3) isozyme (*7*, *8*). Thus, an interesting difference exists between individual isozymes that have similar structures. The amino acid sequences reveal that the class 3 isozyme is 40% identical to either the class 1 or class 2 isozyme and that the class 1 isozyme is 70% identical to the class 2 isozyme (*9*). The three isozymes also share similar three-dimensional structures (*10*−*13*). For either the class 1 or class 2 isozyme, the subunit structure was determined to be a binary complex with NAD^+ in the presence of Mg^{2+} ions (*10*−*12*). The structure shows that the ion interacts with the pyrophosphate group of NAD^+. For the class 3 isozyme, the structure of the binary complex was determined in the absence of a divalent ion, so it is not known if any ion binds to the enzyme (*13*).

Each isozyme catalyzes the same basic chemical sequence of events as depicted in Figure 1. The rate-limiting step of each isozyme, however, appears to be different. It is coenzyme dissociation (k_9) for the class 1 isozyme (*14*), deacylation (k_7) for the class 2 isozyme (*15*, *16*), and hydride transfer (k_5) for the class 3 isozyme (*17*), as depicted (Figure 1). While employing site-directed mutagenesis with ALDH2, we found point mutations that changed the rate-limiting step of the enzyme from deacylation to hydride transfer (*3*). One of the mutants, E399Q, had a lower dehydrogenase activity that was no longer enhanced by the presence of Mg^{2+} ions when compared with that of the native enzyme. This implies that the only form of the enzyme that was activated by the metal ions was the isozyme whose rate-limiting step was deacylation, a general base-catalyzed step.

Previous studies have not fully examined the effect of Mg^{2+} ions on individual steps catalyzed by the same isozyme. Though it appeared that the metal ions caused the class 1 isozyme to bind NADH tightly (*6*), it is not known if they would do the same with the class 2 isozyme. Similarly, while it was possible to determine that Mg^{2+} ions caused the deacylation rate to be increased for the class 2 enzyme (*3*), it is not known if the metal ions would cause this non-rate-limiting step to become faster with the class 1 enzyme. Here, we examined the effect of Mg^{2+} ions on a number of steps catalyzed by ALDH1 and ALDH2. These include hydride transfer, deacylation, coenzyme dissociation, and the initial formation of the covalent adduct with the enzyme. The latter step is not rate-limiting for any dehydrogenase reaction but is when the hydrolysis of *p*-nitrophenyl acetate is catalyzed

† This research was supported by NIH Grant AA05812. This is paper 17655 from the Purdue University Agriculture Experiment Station.

* To whom correspondence should be addressed. Telephone: (765) 494-1650. Fax: (765) 494-7897. E-mail: Hweiner@purdue.edu.

‡ Purdue University.

§ These authors contributed equally to this study.

|| Indiana University School of Medicine.

[1] Abbreviations: ALDH, aldehyde dehydrogenase; ALDH1, human liver cytosolic aldehyde dehydrogenase; ALDH2, human liver mitochondrial aldehyde dehydrogenase; ALDH3, human stomach cytosolic aldehyde dehydrogenase.

10.1021/bi050038u CCC: $30.25
Published on Web 05/11/2005

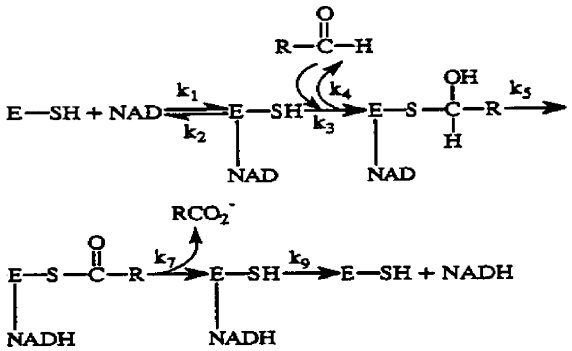

FIGURE 1: Proposed mechanism of the dehydrogenase reaction catalyzed by ALDH.

by ALDH (*15*). The purpose of the study was to try to determine why the metal ion had such diverse effects on isozymes that have very similar three-dimensional structures.

MATERIALS AND METHODS

Chemicals. NAD^+ and NADH were from Sigma. Acetaldehyde, chloroacetaldehyde, benzaldehyde, propionaldehyde, and *p*-nitrophenyl acetate were from Aldrich. α-[^{2}H]Benzaldehyde (C_6H_5CDO) was from Cambridge Isotope Laboratories, Inc. [^{2}H]Acetaldehyde (CD_3CDO) was from Aldrich. [^{35}S]dATP was from Amersham. T_4 DNA ligase and restriction enzymes were from either New England Biolabs or Promega. The Minipreps DNA purification kit was from Biolabs. The Mutagene M13 *in vitro* mutagenesis kit was from Bio-Rad. The thermocycler sequencing kit was from Epicentre Technologies.

Cells and Plasmids. Native or mutant ALDH1 and ALDH2 cDNAs were cloned into pT7-7 plasmids and expressed in *Escherichia coli* strain BL21(DE3) (pLysS) as previously described (*18*, *19*). The ALDH1 E339Q mutant was created with mutagenic primers and the Mutagene M13 *in vitro* mutagenesis kit, based on the procedure described by Kunkel et al. (*20*). After the mutation in M13 had been ascertained by DNA sequencing, the mutant sequence was ligated into the pT7-7 plasmid. The recombinant plasmid was cloned into BL21 cells, amplified, and sequenced to confirm the presence of the mutant sequence.

*Expression in E. coli and Purification of the Native and Mutant Enzyme*s. All enzymes were expressed and purified as described previously (*19*, *21*). Briefly, recombinant enzymes were purified by protamine sulfate treatment (1.25 mg/mL) followed by a DEAE-cellulose column and *p*-hydroxyacetophenone (HAP) affinity chromatography. The purified enzymes were homogeneous as indicated by SDS−PAGE (*22*). Fractions containing individual purified enzymes were pooled and concentrated by Centricon centrifugal filters (Amicon). Prior to subsequent characterization, the concentrated enzymes were stored in 50% glycerol at −20 °C and found to be stable for at least 6 months.

Fluorescence and Absorbance Assay for the Dehydrogenase Activity. The dehydrogenase activity assays were performed by measuring the rate of increase in the fluorescence or absorbance of NADH formation in 50 mM sodium phosphate or 25 mM Hepes (pH 7.4) at 25 °C. The K_m and V_m values for NAD^+ were determined for ALDH2 and ALDH1 in the presence of 14 and 140 μM propionaldehyde, respectively. The K_m and V_m values for propionaldehyde were determined in the presence of 1 mM NAD^+. The dissociation constants for NAD^+ (K_{ia}) were determined by bisubstrate kinetic analysis (*23*). The dissociation constants of NADH (K_{iq} or k_{10}/k_9) were determined as inhibition constants using NADH as a competitive inhibitor against NAD^+. The K_{iq} for NADH was determined with a constant concentration of propionaldehyde of 14 and 140 μM for ALDH2 and ALDH1, respectively, and a varied concentration of NAD^+. Linear regression analysis of a double-reciprocal plot or a Dixon plot was used for calculating the value of K_{iq} (*24*). The buffer and Mg^{2+} ion concentrations used are indicated for each experiment.

Displacement Experiments. The NADH was displaced from the binary enzyme−NADH complex by adding an excess of NAD^+ as indicated below:

$$\text{E}-\text{NADH} \underset{k_{10}}{\overset{k_9}{\rightleftharpoons}} \text{E} + \text{NADH}$$

$$\text{E} + \text{NAD}^+ \xrightarrow{k_1} \text{E}-\text{NAD}^+$$

When the concentration of NAD^+ is very high, the k_1-[NAD^+] product is much greater than k_{10}[NADH]. Under these conditions, the rate of decrease in fluorescence caused by the release of NADH from the E−NADH complex to form the less fluorescent free NADH will be determined by the rate of dissociation of the E−NADH complex, as shown above. The rate of NADH dissociation (k_9) can be calculated as a first-order rate, by plotting it against time the logarithm of the difference between the fluorescence at each time and the fluorescence at an infinite time. When the concentration of NAD^+ is high compared to its dissociation constant, the coenzyme is essentially not released from the E−NAD^+ complex during the course of the measurement.

Spectrophotometric Assay for Esterase Activity. The esterase activities of recombinant ALDH1 and ALDH2 were determined by measuring the rate of *p*-nitrophenol formation at 400 nm in 50 mM Pipes (pH 7.4) with 1 mM *p*-nitrophenyl acetate as the substrate. A molar extinction coefficient of 18.3×10^3 M^{-1} cm^{-1} at 400 nm for *p*-nitrophenolate was used for calculating its rate of formation.

Determination of the Primary Deuterium Isotope Effect. ALDH activity was determined in 25 mM Hepes buffer (pH 7.4) at 25 °C. The isotope effect was determined by comparing the V_m using acetaldehyde, [^{2}H]acetaldehyde, benzaldehyde, or α-[^{2}H]benzaldehyde.

Determination of Protein Concentrations. A protein assay kit (Bio-Rad) with bovine serum albumin as a standard was used for determining protein concentrations.

RESULTS

Rate-Limiting Step for ALDH1. It has been suggested that NADH dissociation could be rate-limiting for the sheep liver class 1 ALDH (*14*). We have shown in the past that comparing the rate of oxidation between chloroacetaldehyde and acetaldehyde was a good way to determine if k_3 or k_5 (Figure 1) was the rate-limiting step (*25*). The specific activity for the oxidation of chloroacetaldehyde by ALDH1 was found to be essentially the same as that with acetaldehyde, consistent with coenzyme dissociation being rate-limiting for ALDH1. Mg^{2+} ions, in a dose-dependent manner, caused a decrease in ALDH1 activity at pH 7.4 (Figure 2). The activity dropped markedly as the ion concentration

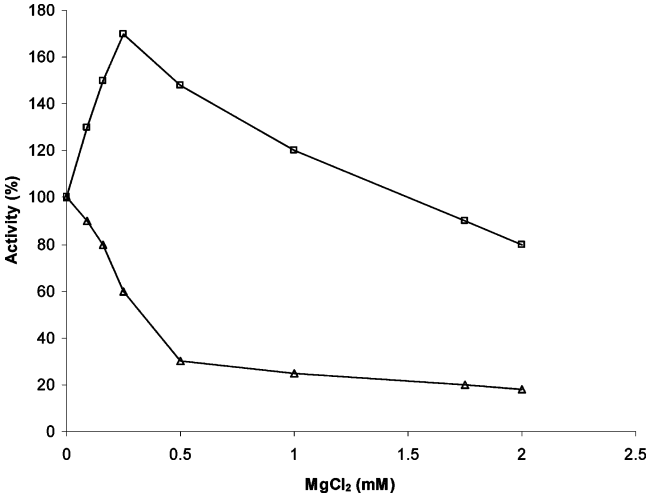

FIGURE 2: Effect of the Mg^{2+} ions on human liver cytosolic aldehyde dehydrogenase, ALDH1, using propionaldehyde under V_m conditions at both pH 7.4 (△) and 5.5 (□). Phosphate buffer (50 mM) and NAD^+ (1 mM) were used.

Table 1: Primary ^2H Isotope Effect on the Native and Mutant Forms of Human Liver Class 1 Aldehyde Dehydrogenase (ALDH1)

	V_H/V_D[a]	
enzyme	acetaldehyde	benzaldehyde
ALDH1		
native	1	1
E399Q mutant	3	1
ALDH2[b]		
native	1	1
E399Q mutant	2.5	1
ALDH3[c]		
native	ND[d]	2.1
E333Q mutant	ND[d]	NA[e]

[a] V_H refers to the dehydrogenase activity (nanomoles per minute per milligram of protein) when acetaldehyde or benzaldehyde was used as the substrate. V_D refers to the dehydrogenase activity when α-[^2H]acetaldehyde or α-[^2H]benzaldehyde was used as the substrate. [b] Human liver class 2 aldehyde dehydrogenase (from ref *3*). [c] Human stomach class 3 aldehyde dehydrogenase (from ref *17*). [d] No available data. [e] No measurable activity.

increased to ~0.5 mM, as would be expected for an ALDH whose rate-limiting step was not deacylation or hydride transfer but was coenzyme dissociation.

The E399Q mutant of ALDH1 was made in hopes that the rate-limiting step of the mutant would change as it did for ALDH2. No primary isotope effect was found for the native enzyme with either [^2H]acetaldehyde or α-[^2H]-benzaldehyde, indicating that hydride transfer was not the rate-limiting step for the native enzyme (Table 1). The ALDH1 mutant, however, exhibited a primary isotope effect on aldehyde oxidation when [^2H]acetaldehyde was the substrate. Analogous to what was found with the ALDH2 mutant (*3*), the ALDH1 mutant exhibited no primary isotope effect when α-[^2H]benzaldehyde was the substrate. This implies, like it did for the ALDH2 mutant, that hydride transfer becomes rate-limiting for the ALDH1 mutant when acetaldehyde was the substrate but not when aromatics were employed.

While 0.5 mM Mg^{2+} ions inhibited the native ALDH1 by ~85% at pH 7.4 (Figure 2), the metal ions did not seem to affect the ALDH1 mutant even at 1 mM. It appears that the ions, though binding to NAD^+, do not affect k_{cat} values of enzyme forms whose rate-limiting step is not deacylation.

Table 2: Effect of Mg^{2+} Ions on the Kinetic Constants of Human Liver Class 1 (ALDH1) and Class 2 (ALDH2) Aldehyde Dehydrogenases[a]

	ALDH1		ALDH2	
kinetic constant	without Mg^{2+}	with Mg^{2+}	without Mg^{2+}	with Mg^{2+}
$K_m(NAD^+)$ (μM)	6.2	0.3	41	120
K_m(propionaldehyde) (μM)	5.2	1.2	0.2	0.2
k_{cat} (min^{-1})	80	21	190	370
K_{ia} (μM)	8.6	0.7	49	39
K_{iq} (μM)[b]	52	19	140	12

[a] Assays were conducted in 50 mM sodium phosphate buffer (pH 7.4) using 0 or 2 mM $MgCl_2$. Constants are from eq 1. [b] The K_{iq} value was determined as an inhibition constant for NADH and not from the primary data used in eq 1. Assays for K_{iq} were conducted in 25 mM Hepes (pH 7.4), using 0 or 2 mM $MgCl_2$ for ALDH1 and 0 or 5 mM $MgCl_2$ for ALDH2.

Effect of Mg^{2+} Ions on the Steady-State Kinetic Constants. Traditional two-substrate kinetic techniques (*26*) were used to determine a number of kinetic constants for both ALDH1 and ALDH2. The velocity data were fitted to the standard bi-bi ordered sequential equation in the absence of products (eq 1). Primary double-reciprocal data were used to produce secondary plots from which the constants were calculated.

$$v = \frac{k_{cat}[E][A][B]}{K_{ia}K_B + K_a[B] + K_B[A] + [A][B]} \quad (1)$$

where [A] and [B] refer to the NAD^+ and acetaldehyde concentrations, respectively. In addition, the effect of NADH as a competitive inhibitor against NAD^+ was studied. Table 2 summarizes the data obtained for both isozymes in the presence or absence of Mg^{2+} ions.

K_{ia}, the dissociation constants for NAD^+, and K_{iq}, measured as the inhibition constant for NADH acting as a competitive inhibitor, each decreased in the presence of Mg^{2+} ions for both isozymes. This implies that the presence of Mg^{2+} ions caused the coenzyme to bind more tightly to each isozyme.

Effect of Mg^{2+} Ions on the Displacement of NADH from the Enzyme. To directly measure the influence of Mg^{2+} ions on the dissociation of NADH from the enzyme−NADH binary complex, a displacement experiment was performed by taking advantage of the fact that NADH is more fluorescent when bound to the enzyme (*14*). The enzyme was mixed with NADH in a fluorometer, and excess NAD was added. As NADH dissociated from the enzyme, NAD^+ would bind. Figure 3 shows a plot of the decrease in NADH fluorescence as a function of time in the presence and absence of Mg^{2+} ions. With ALDH1, the velocity for NADH dissociation, which would be equivalent to k_9 in Figure 1, decreased ~10-fold in the presence of 2 mM Mg^{2+} ions. With ALDH2, 2 mM Mg^{2+} ions had no significant effect on the velocity for NADH displacement. If, however, 5 mM Mg^{2+} ions were used, then the velocity was found to decrease ~3-fold. Thus, Mg^{2+} ions appeared to cause NADH to bind more tightly to both isozymes.

Effect of Mg^{2+} Ions on the Deacylation Step. As mentioned above, chloroacetaldehyde is oxidized more rapidly than acetaldehyde when the rate-limiting step involves nucleophilic attack, as would be found for deacylation (k_7) or formation of the thio−hemiacetal intermediate (k_3). Also, it

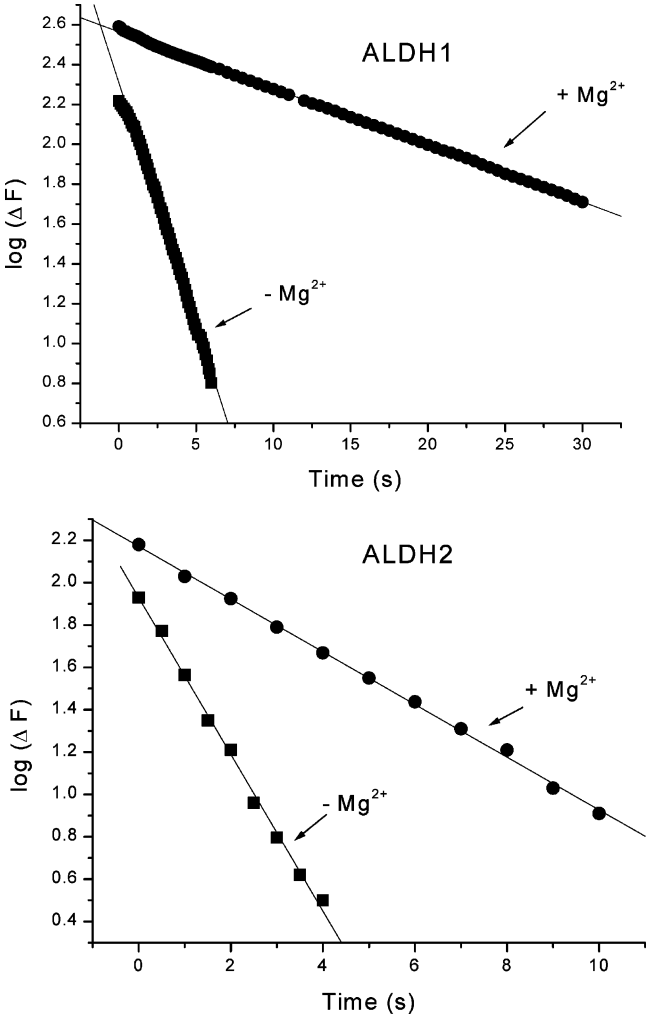

FIGURE 3: Effect of Mg^{2+} ions on displacement of NADH from the E−NADH binary complex. NADH was displaced from the binary ALDH−NADH complex by injecting at time zero an excess of NAD^+ (2.4 mM) in a cuvette containing ~3 μM enzyme and ~10 μM NADH in the presence and absence of 2 mM Mg^{2+} ions for human liver cytosolic aldehyde dehydrogenase (ALDH1) and 5 mM Mg^{2+} ions for human liver mitochondrial aldehyde dehydrogenase (ALDH2), respectively. The decrease in NADH fluorescence was monitored as a function of time in 50 mM Pipes buffer (pH 7.4).

has been shown that Mg^{2+} ions increased the rate of oxidation of acetaldehyde for the mammalian class 2 ALDHs (*1*−*3*). These findings were reconfirmed with ALDH2 (Figure 4). We, however, did not expect to have found that inhibition of acetaldehyde oxidation started to occur at much higher concentrations of Mg^{2+} ions. The oxidation of chloroacetaldehyde was not enhanced by the presence of low concentrations of Mg^{2+} ions but was actually inhibited at all ion concentrations. The inhibition pattern with either aldehyde mimicked the ion effect observed for ALDH1 whose rate-limiting step was NADH dissociation.

The inhibition of ALDH2 observed at high Mg^{2+} ion concentrations with acetaldehyde, or at all concentrations with chloroacetaldehyde, could be the result of the rate-limiting step ultimately becoming coenzyme dissociation. This could occur if at low concentrations of ion there was an increase in the rate-limiting deacylation step (k_7). At higher concentrations, though, the metal could retard the dissociation of NADH form the enzyme so inhibition would

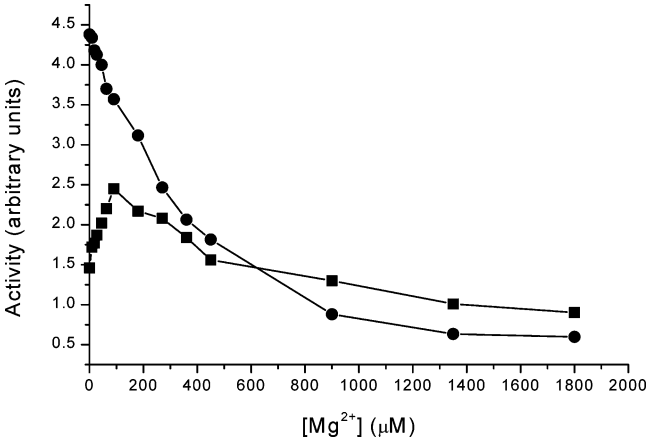

FIGURE 4: Effect of the Mg^{2+} ions on human liver mitochrondial aldehyde dehydrogenase (ALDH2) using V_m conditions for both acetaldehyde (■) and chloroacetaldehyde (●). Pipes buffer (50 mM, pH 7.4) was used.

be found. The rate of NADH dissociation from ALDH2 (k_9) or its inhibitory constant (K_{iq}) is affected by Mg^{2+} ions (Table 2), consistent with the explanation.

While investigating the effect of pH on the steady-state turnover for ALDH1, we observed that the enzyme not only oxidized chloroacetaldehyde better than acetaldehyde in acidic buffers but also showed a pre-steady-state burst of NADH formation when propionaldehyde was used as a substrate (data not shown). These findings implied that the rate-limiting step of the enzyme could have become deacylation (k_7) and that its activity could be enhanced by Mg^{2+} ions. We therefore investigated the effect of Mg^{2+} ions on ALDH1 at pH 5.5. As predicted, the result obtained with ALDH1 was analogous to what was found for ALDH2 at pH 7.4 (Figure 2). The enzyme activity increased with low concentrations of Mg^{2+} ions but decreased at high concentrations of the ions. It appears, then, that Mg^{2+} ions can enhance the general base-catalyzed deacylation step for both ALDH1 and ALDH2. Enhancement was only observed under conditions where a step requiring general base catalysis was rate-limiting. Apparently in the presence of high concentrations of ions, coenzyme release again becomes rate-limiting, accounting for the observed inhibition.

Effects of Mg^{2+} Ions on the Acylation Step. The step remaining to be investigated was the one governed by k_3, binding of aldehyde to the active site cysteine to form the thio−hemiacetal intermediate. The presence of Mg^{2+} ions did not greatly affect the K_m of either isozyme for propionaldehyde (Table 2); thus, it could be assumed that k_3 might not be affected. To look more closely at that step, the esterase activity of the isozymes was investigated (*15*) since it is not possible to conveniently assess aldehyde binding. It was previously shown that the rate-limiting step for the esterase reaction was acylation with ALDH2 (*25*). This step is analogous to aldehyde binding in that for each a covalent thio adduct is formed. We found no pre-steady-state burst of *p*-nitrophenol when either ALDH isozyme was assayed for esterase activity with *p*-nitrophenyl acetate (data not shown). Also, neither isozyme exhibited any increase in esterase activity in the presence of Mg^{2+} ions (Figure 5). This would be expected, since in the three-dimensional structure of either isozyme, the metal ion appeared to bind to only the coenzyme. In the presence of NAD^+ or NADH,

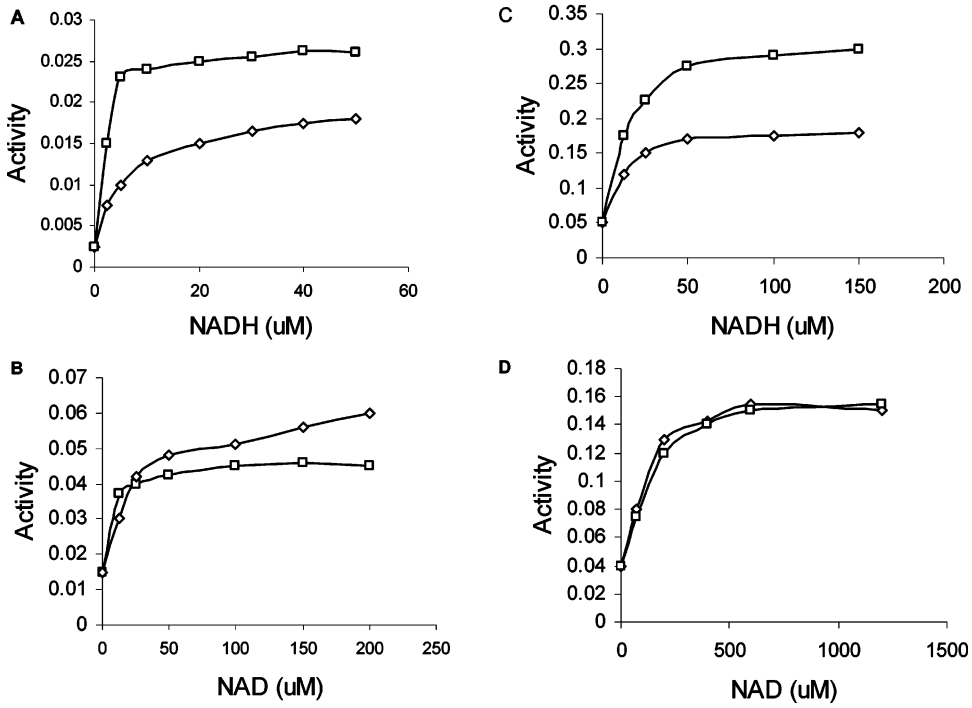

FIGURE 5: Mg^{2+} ion effects on NADH and NAD^+ activation of *p*-nitophenyl acetate hydrolysis by human liver cytosolic aldehyde dehydrogenase (ALDH1) (A and B) and mitochrondial aldehyde dehydrogenase (ALDH2) (C and D). The symbols correspond to 0 (◇) and 3 mM (□) Mg^{2+} ions. Pipes buffer (50 mM, pH 7.4) was used. Activity is presented in arbitrary units.

each isozyme showed an increase in esterase activity. Mg^{2+} ions affected differently the coenzyme-activated activity, depending upon which form of the coenzyme was present. The NADH-activated activity was further increased by the presence of Mg^{2+} ions for each isozyme. In contrast, the metal ions did not affect the NAD^+-activated activity of ALDH2 while lowering that of ALDH1.

It was argued that the presence of coenzyme increased the nucleophilicity of Cys302 responsible for acylation (*27*). Marshall and Branlant (*28*) reported that coenzyme binding was able to induce a reorientation of the side chain of Cys302 that rendered it more accessible and more reactive, at neutral pH. Therefore, if all Mg^{2+} ions did was to enhance the binding of coenzyme, one would expect that in the presence of Mg^{2+} ions, the esterase activity would not increase but it would take less coenzyme to cause the activation. This was not what was observed for either isozyme in the presence of NADH. As shown in Figure 5, not only was the esterase activity of the isozyme increased but the NADH activation occurred at a lower concentration than it did in the absence of Mg^{2+} ions.

DISCUSSION

Both ALDH1 and ALDH2 employ the same mechanistic pathway for aldehyde oxidation, though they differ in which step is rate-limiting. It is NAD^+ (*14*) dissociation for ALDH1 and deacylation for ALDH2 (*15*, *16*). Earlier studies indicated that Mg^{2+} ions inhibited the activity of ALDH1 (*6*), while enhancing that of ALDH2 (*2*, *3*). Since the effects of Mg^{2+} ions were investigated under V_m conditions, it seemed that the ions retarded dissociation of NADH from ALDH1 and enhanced deacylation in ALDH2. In this study, we show that Mg^{2+} ions affected similarly the same steps in ALDH1 and ALDH2, but all the effects could not be detected under V_m conditions since each isozyme had a different rate-limiting step.

The hydride transfer step when acetaldehyde was the substrate for either isozyme was not affected by Mg^{2+} ions. This was initially demonstrated using an ALDH2 mutant whose rate-limiting step had been converted from deacylation to hydride transfer (*3*). It was next shown that the metal ions had no effect on the velocity of ALDH3, a natural enzyme with hydride transfer as the rate-limiting step (*17*). Here, we show that the E3993Q mutant of ALDH1 behaved like the ALDH2 mutant with respect to the rate-limiting step. The possible role of Glu399 was apparent from an examination of recent crystallographic data for different complexes between ALDH2 and NAD(H) (*29*). As shown in Figure 6, the carboxyl groups of Glu399 and the hydroxyl groups of the nicotinamide ribose are close enough to form two hydrogen bonds when NAD^+ is in an extended conformation which is ideal for hydride transfer. Mutation to glutamine appears to weaken the hydrogen bonding capabilities of the enzyme, either because glutamine prefers an alternate conformation (Figure 6) or because stable binding of the nicotinamide ribose hydroxyl groups requires that the side chain of Gln399 accept hydrogen bonds. Disruption of the hydrogen bonding could affect the formation of an extended NAD^+ conformation, causing the ALDH2 mutant to be less able to transfer the hydride ion from the substrate to NAD^+. The occurrence of an extended conformation of NAD^+ in ALDH1 has been suggested, on the basis of NMR and fluorescence spectroscopic studies (*30*). To help interpret the role of Glu399 in the ALDH1 isozyme, we relied on the crystal structure of the class 1 ALDH from sheep liver (*10*). Since ALDH1 and the sheep enzyme are more than 90% identical in sequence, it would be expected that both share the same crystal structure. The sheep enzyme structure shows

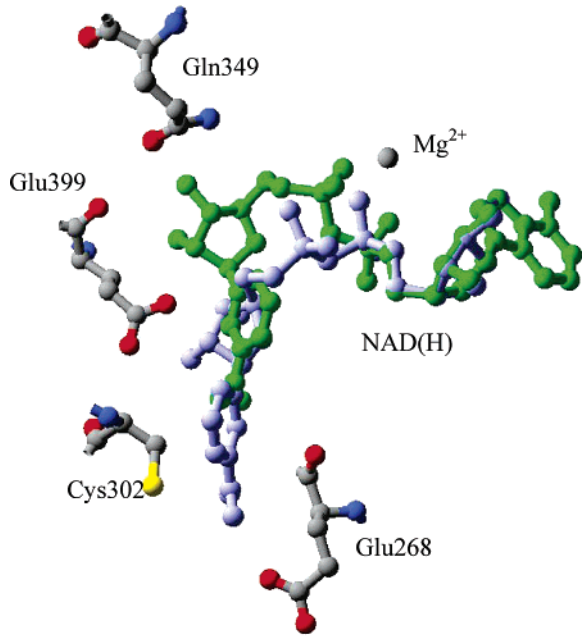

FIGURE 6: Interactions between the different coenzyme conformations in ALDH2. This figure shows the relative positions of Gln349, Glu399, Cys302, and Glu268 with respect to that of NAD^+ at the active site of ALDH2. The nicotinamide ring in the hydrolysis and the hydride transfer conformation are colored green and pale blue, respectively. The crystallographically observed position of Mg^{2+} when bound to the hydrolysis position is also shown as a gray sphere.

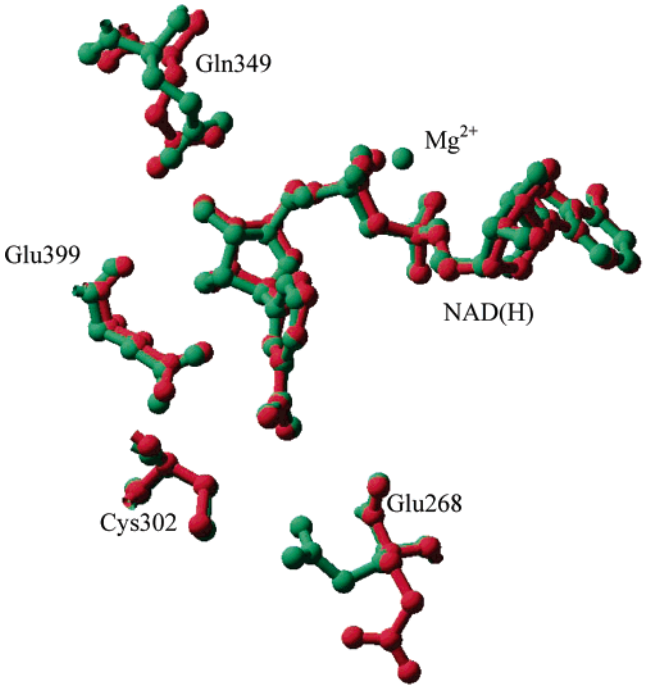

FIGURE 7: Comparison of active site residues in ALDH1 and ALDH2. The active site of sheep liver class 1 ALDH (PDB entry 1BXS, colored red) and the active site of ALDH2 (PDB entry 1O02, colored green) were overlaid on the basis of the orientations of the two tetramers using the DeepView/Swiss-PDB Viewer program (http://us.expasy.org/spdbv/). An alternate conformation for Glu268 in ALDH2 is illustrated here to show its ability to move toward Cys302 following coenzyme isomerization. The bound cofactors and Mg^{2+} ion in ALDH2 are also included to highlight the similarities between the two isozymes.

a contracted conformation of NAD^+ with the hydroxyl groups of the nicotinamide ribose hydrogen bonding the carboxyl groups of Glu399 and Gln349. Hydrogen bonds formed between NAD^+ and the same amino acids have been reported in one of the crystal structures of ALDH2 when NAD^+ was in a contracted conformation (*29*). We superimposed the sheep enzyme structure onto the ALDH2 structure, using a DeepView/Swiss-PDB Viewer program made available at http://us.expasy.org/spdbv/. The overlapping structures (Figure 7) showed that NAD^+, Glu399, and Gln349 of one fitted well with the corresponding members of the other except for the side chains of the Gln residues which appeared to be in different orientations. On the basis of the structures presented in Figures 6 and 7, it was clear that shifting of NAD^+ from a contracted conformation to an extended one would be expected to disrupt the hydrogen bond between Gln349 and the nicotinamide ribose and generate a second hydrogen bond between the nicotinamide ribose and Glu399.

The only step that was not directly investigated was the one governed by k_3, binding of aldehyde to produce the thio−hemiacetal intermediate. On the basis of the study of the esterase reaction, it was evident that like k_5, the magnitude of k_3 was independent of Mg^{2+} ions in the absence of the coenzyme. Our results on the esterase reaction were consistent with those reported in an earlier study (*6*), except for the effect of Mg^{2+} ions on the NAD^+-activated esterase activity of ALDH1. The reason for this is not clear. Here, we used a Mg^{2+} ion concentration higher than that in the earlier study, to obtain a decrease in the NAD^+-activated esterase activity of ALDH1.

The differential effects of the Mg^{2+} ions on ALDH1 and ALDH2 with respect to NAD^+ activation could be related to the fact that the nicotinamide portion of the coenzyme exists in different conformations. When binding to either isozyme, the adenine portion is immobile while the nicotinamide ring can sample different conformations (*30*). Further, the presence of Mg^{2+} ions appears to affect the mobility of the nicotinamide ring. The metal ions tighten the binding of NAD^+ to either isozyme as shown by the decreased K_{ia} values with the effect being much greater for ALDH1. When Mg^{2+} ions are present, crystallographic evidence has shown that the nicotinamide ring of NAD^+ is preferentially located adjacent to Cys302 which would sterically restrict the binding of the ester and the release of the leaving group following acylation. Thus, the esterase reaction is not enhanced in ALDH2 or actually is inhibited in ALDH1 when Mg^{2+} ions are present. The difference in these effects could be due to differing residency times for the hydrolysis versus the hydride transfer conformations between the two isozymes when Mg^{2+} ions are present. In contrast to what was found with NAD^+, Mg^{2+} ions when bound to the enzyme−NADH complex appear to activate both k_3 and k_7. The esterase reaction, governed by k_3, of either isozyme was activated when Mg^{2+} ions were included in the assays containing NADH. From the K_{iq} values, it can be seen that NADH binds more tightly to either isozyme in the presence of Mg^{2+} ions. Crystallographic evidence has shown that when Mg^{2+} ions are present, NADH is preferentially bound in the hydrolysis conformation which accords more space near Cys302 for the ester to bind, acylate, and release the leaving group. This conformation also provides access to the acylated enzyme intermediate for the hydrolysis through general base catalysis

from Glu268. Thus, the differential effects of Mg^{2+} ions on the esterase reaction in the presence of an oxidized or reduced cofactor can be explained by the steric requirements for acylation and deacylation at Cys302 and the preferential positions occupied by the oxidized or reduced cofactor in the presence of Mg^{2+} ions.

NADH binds more tightly to the sheep liver class 1 isozyme in the presence of Mg^{2+} ions (*31*). The displacement experiments showed that the presence of Mg^{2+} ions caused NADH to be released more slowly from either isozyme (Figure 3). Although NADH dissociation is not typically rate-limiting for ALDH2, the presence of Mg^{2+} ions does slow the off-velocity of NADH from the binary complex just as it does with ALDH1. In the absence of Mg^{2+} ions, ALDH2 oxidized acetaldehyde 3−4 times more slowly than chloroacetaldehyde. The isozyme exhibited a 2-fold increase in the oxidation rate of acetaldehyde in the presence of Mg^{2+} ions. This could be due to an improved activation of the general base involved in the deacylation rate, a measure of k_7, or acceleration of a partially rate-limiting coenzyme isomerization step that occurs between hydride transfer (k_5) and deacylation (k_7). When chloroacetaldehyde was the substrate for ALDH2, the presence of Mg^{2+} ions actually caused inhibition, not activation as found when acetaldehyde was the substrate. Because of the electron-withdrawing chlorine, the chloroacyl intermediate is most likely being hydrolyzed at a rate that cannot be enhanced further by activating the general base in the presence of Mg^{2+} ions. The presence of the metal ions then does not increase the rate of hydrolysis of the acyl intermediate, but instead acts to inhibit the reaction because the dissociation of NADH from the enzyme ultimately becomes rate-limiting as high concentrations of Mg^{2+} ions cause k_9 to decrease.

It is apparent that Mg^{2+} ions slow NADH dissociation, k_9, for both ALDH1 and ALDH2. To determine if the ions also affect deacylation, k_7, for ALDH1 it was necessary to alter the pH of the reaction. At pH 5.5, the rate-limiting step of ALDH1 changed from k_9 to k_7 as indicated by the observation that chloroactaldehyde was oxidized more rapidly than acetaldehyde. In contrast, at pH 7.4, both substrates were oxidized at the same rate. At the lower pH, Mg^{2+} ions caused the rate of acetaldehyde oxidation of ALDH1 to increase just as it did at pH 7.4 with ALDH2, indicating that Mg^{2+} ions can stimulate the ability of the general base to function in the deacylation reaction with both isozymes, either by increasing its chemical reactivity or by more quickly releasing the steric constraints to general base catalysis within the active site.

We have no explanation for why the rate-liming steps are different for the three major isozymes of mammalian ALDH at pH 7.4. It possibly could be related to the subtle differences in coenzyme binding. For ALDH1 and ALDH2, there appears to be some flexibility in nicotinamide ring binding. With ALDH1, it can be assumed that the dominant conformation is one that favors the action of the general base since the rate-limiting step is not deacylation, k_7, but NADH dissociation, k_9. The opposite can be concluded for ALDH2. It is necessary that the nicotinamide ring in ALDH2 be capable of moving during the catalytic time frame, for if the coenzyme were bound only in the hydride transfer conformation it would not be possible for the general base, Glu268, to function as a general base (*11*). The data presented here make it appear that NAD^+ and NADH do indeed have different effects on the general base-catalyzed deacylation step, especially in the presence of Mg^{2+} ions.

In this study, we show that individual kinetic steps for ALDH1 and -2 are affected differently by the addition of Mg^{2+} ions. With each, the ions had no effect on the initial attack of the active site cysteine on substrate (k_3) or the hydride transfer step (k_5) but did inhibit the dissociation of NADH from the enzyme (k_9). Since the three ALDH isozymes have different rate-limiting steps, it appears that Mg^{2+} ions affect each isozyme differently. At least for the ALDH family, by measuring the effect of Mg^{2+} ions under V_{max} conditions, one can easily determine what might be the rate-limiting step for a new form of the enzyme.

REFERENCES

1. Takahashi, K., and Weiner, H. (1980) Magnesium stimulation of catalytic activity of horse liver aldehyde dehydrogenase. Changes in molecular weight and catalytic sites, *J. Biol. Chem. 255*, 8206−8209.
2. Vallari, R. C., and Pietruszko, R. (1984) Interaction of Mg^{2+} with human liver aldehyde dehydrogenase. I. Species difference in the mitochondrial isozyme, *J. Biol. Chem. 259*, 4922−4926.
3. Ni, L., Sheikh, S., and Weiner, H. (1997) Involvement of Glutamate 399 and Lysine 192 in the Mechanism of Human Liver Mitochondrial Aldehyde Dehydrogenase, *J. Biol. Chem. 272*, 18823−18826.
4. Dickinson, F. M., and Hart, G. J. (1982) Effects of Mg^{2+}, Ca^{2+} and Mn^{2+} on sheep liver cytoplasmic aldehyde dehydrogenase, *Biochem. J. 205*, 443−448.
5. Bennett, A. F., Buckley, P. D., and Blackwell, L. F. (1983) Inhibition of the dehydrogenase activity of sheep liver cytoplasmic aldehyde dehydrogenase by magnesium ions, *Biochemistry 22*, 776−784.
6. Vallari, R. C., and Pietruszko, R. (1984) Interaction of Mg^{2+} with human liver aldehyde dehydrogenase. II. Mechanism and site of interaction, *J. Biol. Chem. 259*, 4927−4933.
7. Wang, S. L., Wu, C. W., Cheng, T. C., and Yin, S. J. (1990) Isolation of high-K_m aldehyde dehydrogenase isoenzymes from human gastric mucosa, *Biochem. Int. 22*, 199−204.
8. Lindahl, R., and Evces, S. (1984) Rat liver aldehyde dehydrogenase. II. Isolation and characterization of four inducible isozymes, *J. Biol. Chem. 259*, 11991−11996.
9. Perozich, J., Nicholas, H., Wang, B. C., Lindahl, R., and Hempel, J. (1999) Relationships within the aldehyde dehydrogenase extended family, *Protein Sci. 8*, 137−146.
10. Moore, S. A., Baker, H. M., Blythe, T. J., Kitson, K. E., Kitson, T. M., and Baker, E. N. (1998) Sheep liver cytosolic aldehyde dehydrogenase: The structure reveals the basis for the retinal specificity of class 1 aldehyde dehydrogenases, *Structure 6*, 1541−1551.
11. Steinmetz, C. G., Xie, P., Weiner, H., and Hurley, T. D. (1997) Structure of mitochondrial aldehyde dehydrogenase: The genetic component of ethanol aversion, *Structure 5*, 701−711.
12. Ni, L., Zhou, J., Hurley, T. D., and Weiner, H. (1999) Human liver mitochondrial aldehyde dehydrogenase: Three-dimensional structure and the restoration of solubility and activity of chimeric forms, *Protein Sci. 8*, 2784−2790.
13. Liu, Z. J., Sun, Y. J., Rose, J., Chung, Y. J., Hsiao, C. D., Chang, W. R., Kuo, I., Perozich, J., Lindahl, R., Hempel, J., and Wang, B. C. (1997) The first structure of an aldehyde dehydrogenase reveals novel interactions between NAD and the Rossmann fold, *Nat. Struct. Biol. 4*, 317−326.
14. Blackwell, L. F., Motion, R. L., MacGibbon, A. K., Hardman, M. J., and Buckley, P. D. (1987) Evidence that the slow conformation change controlling NADH release from the enzyme is rate-limiting during the oxidation of propionaldehyde by aldehyde dehydrogenase, *Biochem. J. 242*, 803−808.
15. Weiner, H., Hu, J. H., and Sanny, C. G. (1976) Rate-limiting steps for the esterase and dehydrogenase reaction catalyzed by horse liver aldehyde dehydrogenase, *J. Biol. Chem. 251*, 3853−3855.

16. Feldman, R. I., and Weiner, H. (1972) Horse liver aldehyde dehydrogenase. II. Kinetics and mechanistic implications of the dehydrogenase and esterase activity, *J. Biol. Chem. 247*, 267−272.
17. Mann, C. J., and Weiner, H. (1999) Differences in the roles of conserved glutamic acid residues in the active site of human class 3 and class 2 aldehyde dehydrogenases, *Protein Sci. 8*, 1922−1929.
18. Jeng, J. J., and Weiner, H. (1991) Purification and characterization of catalytically active precursor of rat liver mitochondrial aldehyde dehydrogenase expressed in *Escherichia coli*, *Arch. Biochem. Biophys. 289*, 214−222.
19. Zheng, C. F., Wang, T. T., and Weiner, H. (1993) Cloning and expression of the full-length cDNAs encoding human liver class 1 and class 2 aldehyde dehydrogenase, *Alcohol.: Clin. Exp. Res. 17*, 828−831.
20. Kunkel, T. A., Roberts, J. D., and Zakour, R. A. (1987) Rapid and efficient site-specific mutagenesis without phenotypic selection, *Methods Enzymol. 154*, 367−382.
21. Ghenbot, G., and Weiner, H. (1992) Purification of liver aldehyde dehydrogenase by *p*-hydroxyacetophenone-sepharose affinity matrix and the coelution of chloramphenicol acetyl transferase from the same matrix with recombinantly expressed aldehyde dehydrogenase, *Protein Expression Purif. 3*, 470−478.
22. Laemmli, U. K. (1970) Cleavage of structural proteins during the assembly of the head of bacteriophage T4, *Nature 227*, 680−685.
23. Plowman, K. M. (1972) *Enzyme Kinetics*, McGraw-Hill, New York.
24. Farres, J., Wang, X., Takahashi, K., Cunningham, S. J., Wang, T. T., and Weiner, H. (1994) Effects of changing glutamate 487 to lysine in rat and human liver mitochondrial aldehyde dehydrogenase. A model to study human (Oriental type) class 2 aldehyde dehydrogenase *J. Biol. Chem. 269*, 13854−13860.
25. Wang, X., and Weiner, H. (1995) Involvement of glutamate 268 in the active site of human liver mitochondrial (class 2) aldehyde hydrogenase as probed by site-directed mutagenesis, *Biochemistry 34*, 237−243.
26. Dalziel, K. (1957) Initial steady-state velocities in the evaluation of enzyme-coenzyme substrate reaction mechanisms, *Acta Chem. Scand. 11*, 1706−1723.
27. Takahashi, K., and Weiner, H. (1981) Nicotinamide adenine dinucleotide activation of the esterase reaction of horse liver aldehyde dehydrogenase, *Biochemistry 20*, 2720−2726.
28. Marchal, S., and Branlant, G. (1999) Evidence for the chemical activation of essential Cys-302 upon cofactor binding to non-phosphorylating glyceraldehyde 3-phosphate dehydrogenase from *Streptococcus mutans*, *Biochemistry 38*, 12950−12958.
29. Perez-Miller, S. J., and Hurley, T. D. (2003) Coenzyme isomerization is integral to catalysis in aldehyde dehydrogenase, *Biochemistry 42*, 7100−7109.
30. Hammen, P. K., Allali-Hassani, A., Hallenga, A. K., Hurley, T. D., and Weiner, H. (2002) Multiple conformations of NAD and NADH when bound to human cytosolic and mitochondrial aldehyde dehydrogenase, *Biochemistry 41*, 7156−7168.
31. Dickinson, F. M., and Haywood, G. W. (1986) The effects of Mg^{2+} on certain steps in the mechanisms of the dehydrogenase and esterase reactions catalysed by sheep liver aldehyde dehydrogenase. Support for the view that dehydrogenase and esterase activities occur at the same site on the enzyme, *Biochem. J. 233*, 877−883.

BI050038U